An ultrasonic pulsed Doppler balloon catheter for use in cardiovascular diagnosis

by

Mark Alan Coppess

A Thesis Submitted to the
Graduate Faculty in Partial Fulfillment of the
Requirements for the Degree of
MASTER OF SCIENCE

Major: Biomedical Engineering

Iowa State University
Ames, Iowa

1983

TABLE OF CONTENTS

	Page
LIST OF SYMBOLS	iii
INTRODUCTION	1
LITERATURE REVIEW	5
PROTOTYPE DEVELOPMENT	13
EXPERIMENTAL METHODS AND DATA	19
In Vitro Studies	19
Steady-flow model	20
Pulsatile-flow model	24
In Vivo Studies	31
DISCUSSION OF EXPERIMENTS	45
HEMODYNAMIC EVALUATION AND DEVELOPMENT OF THEORETICAL MODEL	46
Idealized Model	47
Calculations	51
Stenosis Equivalent of Catheter	65
DISCUSSION OF THEORETICAL MODEL RESULTS	71
SUMMARY AND CONCLUSIONS	73
RECOMMENDATIONS FOR FURTHER STUDY	75
LITERATURE CITED	77
ACKNOWLEDGMENTS	79
APPENDIX	80

LIST OF SYMBOLS

A	pressure gradient in the entrance region
a_0	cross-sectional area of the vessel
a_1	minimum cross-sectional area of the stenosis
A_0	cross-sectional area of the vessel
A_1	cross-sectional area of the catheter
A_a	cross-sectional area of the annulus
B	pressure gradient in the expansion region
d_0	diameter of the unobstructed vessel
d_1	minimum diameter of the stenosis
D_0	diameter of the vessel
D_1	diameter of the catheter
D_h	hydraulic diameter
f	fully developed friction factor
K	entrance region pressure drop coefficient
K_t	dimensionless coefficient
K_v	dimensionless coefficient
ℓ	axial distance from entrance of vessel
ℓ_a	adjusted length of stenosis
ℓ_s	length of stenosis
p_0	mean pressure in entrance region
p_1	mean pressure at a given ℓ
p_2	mean pressure distal to the catheter
p_a	mean pressure in the ascending aorta

Δp	pressure gradient
P_1	mean pressure proximal to the stenosis
P_2	mean pressure distal to the stenosis
ΔP	pressure gradient across the stenosis
Q	mean flow
r_0	radius of the vessel
r_1	radius of the catheter
Re	Reynolds number
$\bar{u}_0$	mean velocity in the vessel
$\bar{u}_1$	mean velocity in the annulus
$\bar{u}_2$	mean velocity distal to the catheter
$\bar{u}_a$	mean velocity in the ascending aorta
$\bar{U}_0$	mean velocity in the unobstructed vessel
$\bar{U}_1$	mean velocity in the stenosis
Z	dimensionless axial distance from the vessel entrance
α	Womersley parameter
μ	blood viscosity
ρ	blood density

INTRODUCTION

Atherosclerotic narrowings of the coronary arteries constitute the most frequent clinical problem in cardiovascular disease in the United States today. Coronary artery bypass surgery is an effective means of treatment of significantly narrowed arteries, and this operation is now one of the most commonly performed surgical procedures. However, the selection of patients for coronary artery bypass surgery is a difficult problem. One of the most important diagnostic factors is the extent and distribution of coronary artery narrowings, as visualized from x-ray dye injection during cardiac catheterization. The severity of coronary artery obstructions is usually assessed visually, and reported as percent diameter or area reduction. It is generally assumed that there is a good correlation between the severity of the stenosis, as judged angiographically, and the reduction in coronary blood flow through the obstruction. Although angiography is a major technique used in assessing coronary narrowings, several studies have shown that angiographic measurements of coronary obstructions of intermediate severity are subject to large inter- and intra-observer variations and may correlate poorly with pathological specimens.

Another method has been developed to investigate the severity of coronary artery narrowings which is based on the phenomenon of reactive hyperemia. Physiologists have long known that the release of a transiently, totally occluded, blood vessel results in a marked overshoot in the blood flow through the vessel. This overshoot response, the so-called reactive hyperemia response, is characteristic of normal vessels. It is diminished, however, as the obstruction in the vessel becomes large, and it is abolished totally with severe obstructions. The measurement of reactive hyperemia provides an indication of the severity of the stenosis, and therefore, is an important tool in the assessment of coronary artery lesions.

The recent development of an ultrasonic Doppler velocity probe which can be coupled to the surface of coronary vessels during cardiac surgery has made possible measurements of coronary reactive hyperemia in man. Studies involving measurements of coronary reactive hyperemia using this probe have shown that the usual method of assessing coronary obstructions by subjective visual interpretation of the arteriogram can lead to erroneous conclusions regarding the physiological significance of coronary lesions. At present, cardiac surgeons are studying the use of

measurements of coronary reactive hyperemia, obtained during surgery, to guide them in decisions regarding bypass grafting of angiographically equivocal obstructive lesions. Although the use of this method is promising, measurements of reactive hyperemia in coronary arteries cannot be done short of open heart surgery. A clinical need therefore, exists for preoperative measurements of reactive hyperemia in coronary arteries.

A clinically applicable approach for the physiological evaluation of coronary lesions in man, by the use of reactive hyperemia, would depend on the solution of three related problems concerned with the development of:

1. A preoperative, nontraumatic method to gain access to the region of the coronary artery containing the obstruction.
2. A safe and convenient stimulus for eliciting the reactive hyperemia response.
3. A method for measuring rapid changes in mean coronary flow.

Research has been initiated to attempt to solve these problems, and the long-range goal of this research is to develop and validate a method for the preoperative determination of the physiological significance of coronary obstructive lesions based on observations of reactive hyperemia.

For the research described in this thesis, the

feasibility of using a balloon catheter, containing an ultrasonic Doppler velocity probe at its tip, to make intraluminal measurements of reactive hyperemia is considered. The design of the Doppler balloon catheter is unique in that during cardiac catheterization it can generate a transient occlusion with the balloon and subsequently measure the ensuing reactive hyperemia response. Specifically, this study will address the following questions:

1. Can a reliable balloon catheter be developed having an ultrasonic Doppler velocity probe at its tip?

2. Is the response of the Doppler balloon catheter linear when measuring phasic and mean velocity?

3. Can the Doppler balloon cathether measure reactive hyperemia, and how does the measurement compare to an extraluminally placed probe?

The present study has been divided into prototype development and testing, and a theoretical hemodynamic evaluation of the effect of the catheter on flow. It is anticipated that information gained in this preliminary study will be of value in developing a method whereby the physiological significance of coronary obstructive lesions can be accurately assessed at the time of cardiac catheterization.

LITERATURE REVIEW

The resting heart extracts most of the oxygen from the coronary blood as it flows through the heart muscle and very little of the heart's oxygen needs can be met by additional extraction of oxygen from the coronary blood. Therefore, the only significant way in which the heart can be supplied with additional amounts of oxygen is through an increase in blood flow, usually referred to as hyperemia. When an artery is completely occluded for a few seconds to a few minutes with a subsequent sudden release of the occlusion, the blood flow increases dramatically to several times resting levels. It remains high for a few seconds to a few minutes depending on the period of occlusion. This phenomenon is referred to as the reactive hyperemia response, or more simply, as reactive hyperemia. Figure 1 is a diagrammatic representation of this type of response. The parameters of interest in evaluating reactive hyperemia are the ratio of mean peak flow to mean resting flow, and the duration of occlusion. Normal coronary arteries have mean peak to resting flow ratios of 4.3 ± 0.9 (S.D.) according to Gould et al. (1974) in dogs, and 5.8 ± 0.6 (S.D.) according to Marcus et al. (1981) in man.

As the obstruction becomes more severe, the mean peak

Figure 1. Diagrammatic representation of the reactive hyperemia response

Figure 2. The effect of obstruction upon mean flow of the reactive hyperemia response of a diseased artery

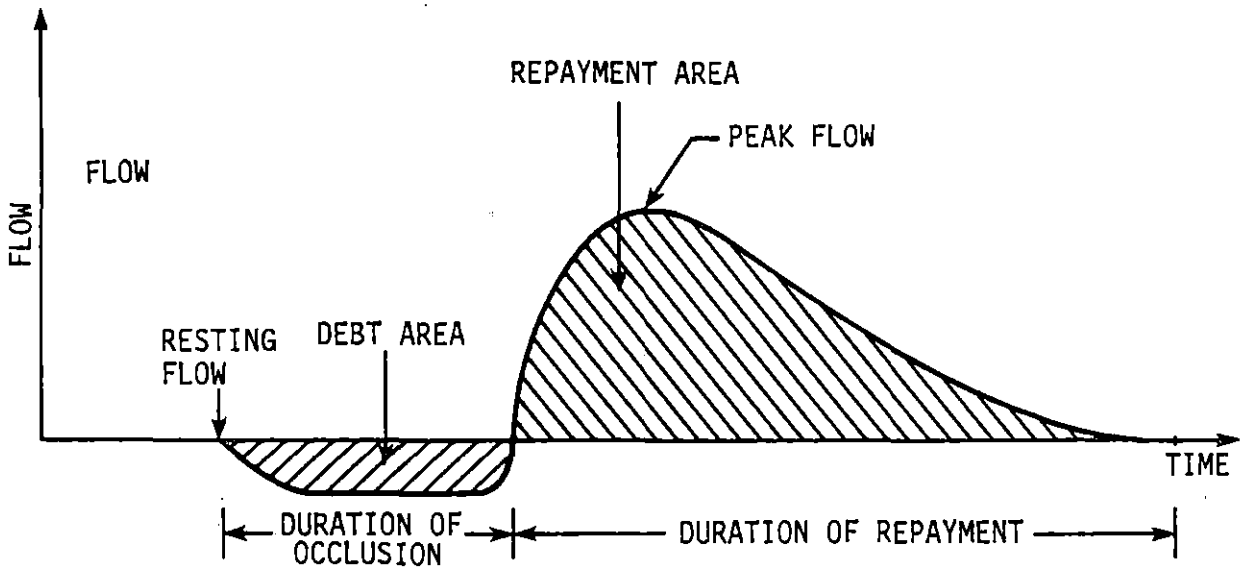

REACTIVE HYPEREMIA

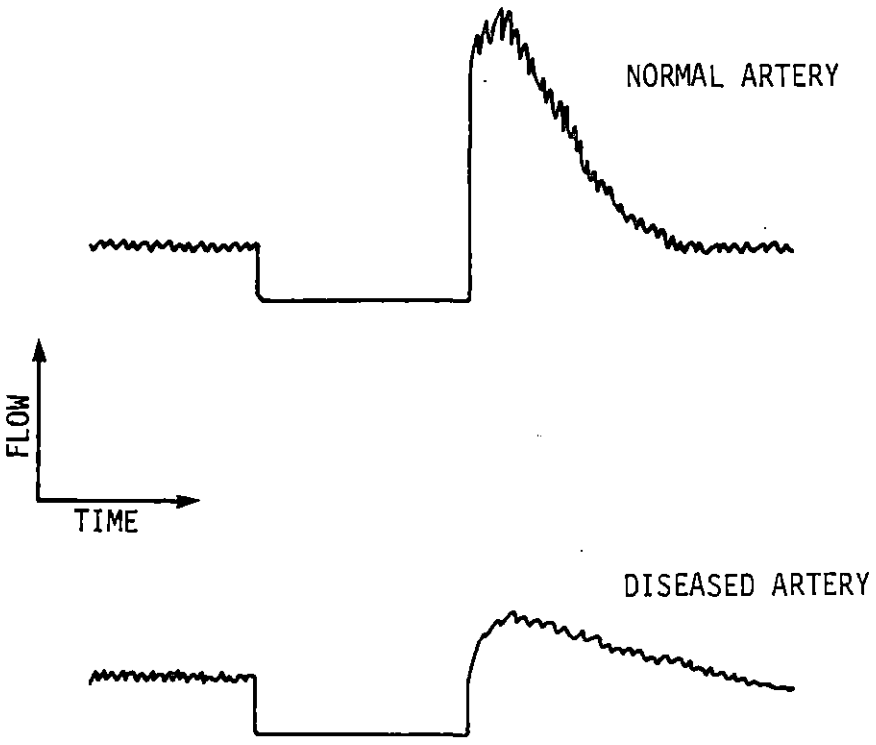

to resting flow ratio diminishes until mean peak flow approaches mean resting flow. Figure 2 illustrates the effect of obstruction on the mean peak flow in a diseased artery. Young et al. (1977) has shown that a coronary stenosis becomes critical sooner at hyperemic flow rates than at resting flow rates. According to Gould et al. (1974), a critical coronary stenosis is defined as a constriction sufficient to prevent an increase in flow over resting values in response to increased myocardial oxygen demands. Gould found that resting coronary blood flow does not decrease until coronary arterial diameter is reduced by 85 percent. However, maximal coronary flow, or coronary flow reserve, begins to decrease with stenosis of 30 to 45 percent of arterial diameter, and the capacity to increase flow over resting levels in response to a vasodilatory stimulus disappears with constriction of 88 to 93 percent of arterial diameter.

Although the coronary arteriogram does provide anatomic definition of coronary lesions, it offers little insight into their hemodynamic consequences short of total or near total occlusion. White et al. (1980) has shown that with coronary obstructions of intermediate severity (10-90%) the correlation between the severity of the stenosis and the vasodilator capacity of the vessel was very poor (r=0.1). The angiographic measurement both

overestimated and underestimated the severity of the lesion as judged from the reactive hyperemia response. More recent studies by Harrison et al. (1981), using the technique developed by Brown et al. (1977) to assess the minimum cross-sectional area by computer-based quantitative coronary angiography, have shown that the correlation between the reactive hyperemia response and the percent area stenosis was poor (r=-0.14). Thus, evaluations of coronary obstructions of intermediate severity by angiography may be insufficient in determining the hemodynamic consequences of such lesions. Therefore, measurements of the mean peak to resting flow ratio obtained from the reactive hyperemia response provides independent, complementary information on the hemodynamic significance of angiographically demonstrated lesions.

Measurements of coronary flow and reactive hyperemia in humans are hampered by methodological problems. Folts et al. (1979) measured phasic coronary flow by placing an electromagnetic flowmeter around the proximal right coronary artery during cardiac surgery. This method has been employed infrequently because it requires extensive surgical dissection for the placement of the flow probe. Several investigators have placed electromagnetic flowmeters on coronary bypass grafts, including Matthews et al. (1971), Bittar et al. (1972), Greenfield et al. (1972) and Olinger

et al. (1976).

Catheters with ultrasonic Doppler piezoelectric crystals mounted at the tip have been in existence for some time. Benchimol et al. (1971) measured phasic coronary velocity in man with a standard coronary catheter with a crystal mounted at its tip. Hartley et al. (1974) reported on the development of a single ultrasonic catheter-tip velocity probe. This system utilized a 1.7 mm diameter piezoelectric crystal with a central 0.5 mm diameter lumen. The crystal was fastened to the tip of a 5 Fr Sones coronary catheter. Cole and Hartley (1977) measured phasic coronary velocity in man using this catheter, which could be introduced into the ostium of the left or right main coronary artery. This technique has not been widely utilized since coronary velocity cannot be measured beyond the main coronary ostia and because the method used to induce ischemia, by injections of contrast media, is difficult to apply quantitatively.

An easy and safe method for recording phasic coronary velocity and reactive hyperemia has been extensively studied and validated in humans by Marcus et al. (1981). This single crystal Doppler velocity probe consists of a small piezoelectric 20 MHz crystal which is bonded to a small transparent plastic suction pad. Two thin stainless steel wires are attached to the opposite side of the

crystal. A small amount of suction is used to couple the Doppler crystal to the coronary vessel at the time of cardiac surgery. A large number of in vitro and in vivo studies have been performed to test the safety of this Doppler system in man and to validate the findings. Animal studies have shown that the probe does not alter myocardial perfusion or cause tissue damage. Changes in mean coronary flow as measured by timed venous outflow or by an electromagnetic flowmeter in the experimental animal are closely correlated ($r=0.9$) to changes in mean coronary velocity using the suction Doppler probe. In these studies, coronary flow was varied over a wide range by employing pharmacologic and physiologic stimuli. The characteristics of reactive hyperemia in the coronary circulation of dogs determined with the suction Doppler probe has been shown to be similar to those obtained simultaneously with an electromagnetic flowmeter. Values for flow velocity can be converted to absolute coronary flow only if the diameter of the vessel and the angle between the flow stream and the beam of ultrasound are known. However, since the ratio of mean peak to resting velocity is approximately equal to the ratio of mean peak to resting absolute flow, it is not essential to know the vessel size or catheter angle in order to determine reactive hyperemia.

According to Gould et al. (1974), there is a need for a convenient, safe, and effective method of stimulating and monitoring brief hyperemia in man to complement angiographic demonstrated lesions with hemodynamic evaluation of such lesions. The problem with existing probes for monitoring reactive hyperemia and phasic velocity in man described is that they either can only be used at the time of cardiac surgery, or, in the case of catheter-tip ultrasonic probes, cannot either generate reactive hyperemia or cannot be subselectively guided in the coronary tree. Therefore, at the present time, there is no established method to preoperatively assess the hemodynamic significance of angiographically demonstrated coronary arterial lesions in man.

PROTOTYPE DEVELOPMENT

In the present study, an attempt has been made to use an ultrasonic catheter-tip velocity probe to measure reactive hyperemia. In addition to being able to measure reactive hyperemia, it was desired that the device be able to generate a temporary occlusion of the vessel. With these design constrictions in mind, a prototype was constructed.

The first prototype utilized a 7 Fr Swan-Ganz thermodilution catheter. This catheter was chosen because it contained electrical wires that extended to within 3 cm of the distal tip. The distal crown of this catheter was removed to the distal segment of the balloon cuff. The thermistor was also removed and additional electrical wires attached. These additional electrical wires were used to connect the thermistor wires to a 1 mm diameter piezoelectric Doppler crystal which was epoxied to the distal tip of the catheter at a 45 degree angle to flow. The 7 Fr Swan-Ganz catheter prototype was abandoned in this present study because it was considered too large in diameter for the coronary tree. Since hemodynamic evaluation of coronary obstructions is the ultimate goal of this research, it was decided that the use of a coronary balloon catheter would be more advantageous.

For the second prototype, a 1 mm diameter ultrasonic piezoelectric crystal was affixed to the distal tip of a 4 Fr U.S.C.I. Gruntzig type 20-30 percutaneous transluminal coronary dilatation (type G) angioplasty catheter. Percutaneous transluminal coronary angioplasty is a non-surgical technique which expands coronary obstructive lesions by the inflation of a precisely constructed polyvinyl chloride balloon attached to the distal tip of a 1.3 mm diameter catheter. These catheters have the following features which are especially desirable for these studies.

1. The catheter can be guided into position subselectively in the coronary tree using a standard preformed guiding catheter.

2. The balloon is constructed so that inflation, even to supra-atmospheric pressures does not increase the dimensions of the balloon. It is resistant to rupture up to 7 atm. pressure.

3. The balloon inflates uniformly around the catheter.

4. The balloon can be inflated with a radio-opaque solutions (i.e., dilute Renografin-76) so that the exact location of the balloon can be identified.

5. Although the length of the balloon is standard (20 mm) several maximal inflation diameters are available (2, 3, and 3.7 mm).

6. The extent of the balloon while deflated is marked with platinum markers so that the proximal and distal extent can be visualized under fluoroscopy during subselective coronary insertion.

7. A distal opening for measuring pressure is available on the side of the catheter, just distal to the balloon.

Because of these advantages, this type of catheter was chosen for the study. The angioplasty dilatation catheters were modified in the following manner:

1. The flexible wire at the distal tip of the catheter was removed to expose the internal lumen.

2. A stainless steel guidewire was introduced from the distal end of the catheter through the pressure lumen and advanced the length of the catheter to its proximal end.

3. Two ultra fine copper wires were soldered to the distal end of the guidewire.

4. The guidewire was withdrawn out the proximal end, bringing the copper wires from the distal to the proximal end of the catheter.

5. A 1 mm diameter 20 MHz piezoelectric crystal was soldered to the distal electrical wires. The crystal (P2T-5A Valtec, Hopkinton) is furnished from the supplier fine-ground with gold plate on each side.

6. The crystal was affixed to the distal end of the catheter with biocompatible epoxy resin and hardener.

7. A special plastic adapter was attached to the proximal end of the pressure lumen and the electrical wires exited through holes in the plastic adapter.

8. The proximal electrical wires were soldered to prongs attached to the outside of the plastic adaptor.

9. The prongs were fixed so that they could be attached by connectors to the pulsed Doppler unit.

A photograph of the Doppler balloon catheter is shown in Figure 3.

Figure 3. The Doppler balloon catheter

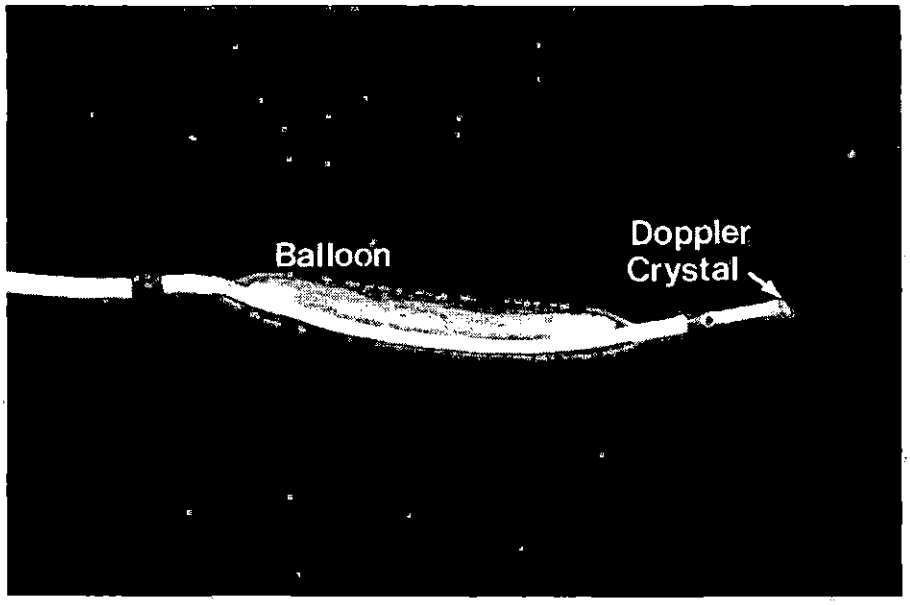
Balloon
Doppler
Crystal

The 20 MHz, ultrasonic directional pulsed Doppler meter is a modification of a circuit developed by Hartley et al. (1974, 1978). Precise details of the modifications in the circuitry have been published by Marcus et al. (1981). This system can accurately measure velocities up to 100 cm/s, ranged anywhere from 0-10 mm away from the crystal. Phasic arterial velocity can be measured with a signal to noise ratio that exceeds 20:1.

EXPERIMENTAL METHODS AND DATA

In Vitro Studies

An in vitro model was devised to test the linearity of the Doppler balloon catheter in both steady and pulsatile flow. A model that would give an indication of the linearity of the Doppler balloon catheter at the range of velocities and range of diameters found in the human coronary circulation was desired. With these parameters in mind, the model was constructed.

Tubes of 2, 3, 4, and 6 mm internal diameter were chosen to test if the presence of the catheter in the lumen would significantly alter the linearity of the device. Measurements obtained from an electromagnetic flowmeter, a 1 mm diameter ultrasonic piezoelectric crystal mounted in a port in the tube wall, and timed collection in a graduated cylinder were used as standards. The fluid used in the in vitro models was a mixture of saline and starch. Saline was used as a conducting medium for the electromagnetic flowmeter, and starch was used as a reflective medium for the ultrasonic probes. The Doppler balloon catheter was always pointed in the same direction as flow in order to simulate coronary artery catheterization.

Steady-flow model

The steady-flow model utilized gravity flow through polyethylene tubes of 2, 3, 4, and 6 mm internal diameter. An electromagnetic flowmeter transducer was located distal to the tip of the Doppler balloon catheter. Figure 4 is a diagram of the steady-flow model. The first steady-flow data were collected by taking numerous random measurements of flow with the electromagnetic flowmeter, Doppler balloon catheter, and by timed collection in the 4 and 6 mm diameter tubes over a velocity range of 0-100 cm/s. The Reynolds number ranged from 276-6816 (assuming the density and viscosity of the solution was essentially that of saline). In order to speed the process of taking data, the electromagnetic flowmeter was first calibrated against flow in a graduated cylinder. Then the results obtained with the Doppler balloon catheter were compared with those obtained with the electromagnetic flowmeter. Correlation coefficients of 0.992 and 0.988 were obtained in the 4 and 6 mm tubes, respectively, when average velocities, as indicated by the Doppler balloon catheter were compared with the corresponding reading from the electromagnetic flowmeter. Table 1 is a listing of velocities obtained by this method. Data were not collected for the 2 and 3 mm diameter tubes because numerous random

Figure 4. Diagram of the steady-flow model

STEADY-FLOW MODEL

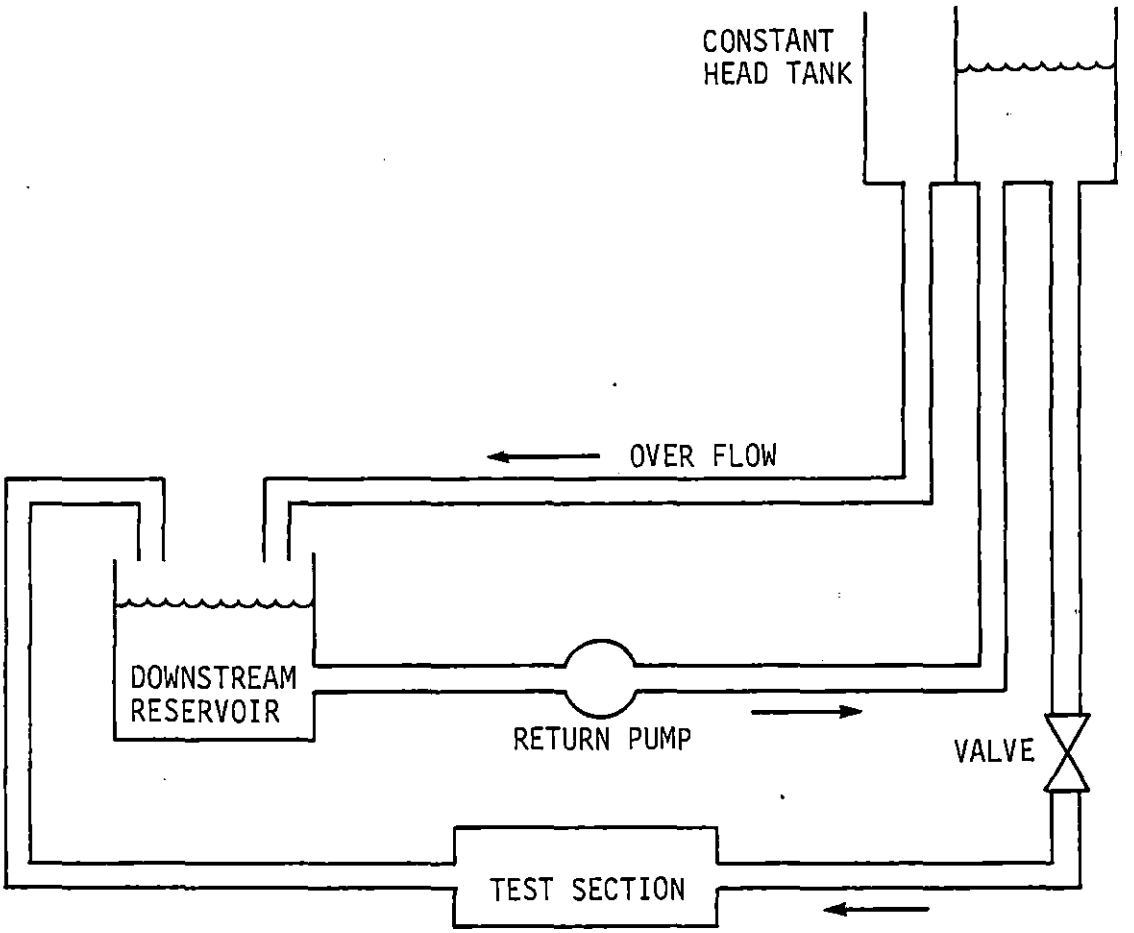

TEST SECTION

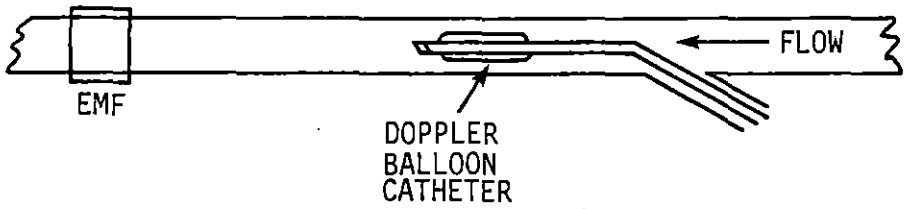

Table 1. Listing of velocities obtained in the steady-flow model by taking measurements with both the Doppler balloon catheter (DBC) and timed collection (Velocity) in the 4 and 6 mm tubes

4 mm I.D.		6 mm I.D.	
DBC[a] (KHz)	Velocity (cm/s)	DBC[a] (KHz)	Velocity (cm/s)
0.00	0.0	0.12	0.0
0.08	9.2	0.14	4.1
0.12	18.0	0.18	11.8
0.18	26.6	0.18	14.0
0.20	31.5	0.20	16.2
0.28	36.5	0.24	19.3
0.36	43.4	0.28	24.2
0.48	54.5	0.30	25.2
0.56	56.7	0.30	27.7
0.64	62.3	0.36	30.0
0.70	67.5	0.50	31.8
0.74	71.6	0.50	35.8
0.82	80.5	0.50	36.6
0.84	83.2	0.56	42.2
0.92	94.9	0.60	43.6
0.98	98.1	0.64	47.8
		0.78	52.0
		0.74	54.4
		0.80	55.8
		0.68	57.0
		0.84	60.9
		0.88	63.7
		0.78	66.8
		0.96	70.7
		0.92	74.6
		0.96	75.9
		0.94	79.2
		1.04	82.0
		0.98	84.0
		1.04	88.2
		1.08	92.0
		1.12	94.0
		1.12	95.1
		1.22	97.0
		1.18	101.4

[a]The readings listed for the Doppler balloon catheter are the averages obtained at those particular velocities.

flows could not be generated.

Next, 8-10 random velocities ranging from 0-100 cm/s were measured by the Doppler balloon catheter and compared with corresponding timed collections in each of the 2, 3, 4, and 6 mm tubes. The Reynolds numbers ranged from 150-7046. The correlation coefficients for these tests were 0.977, 0.996, 0.996, and 0.996 in the 2, 3, 4, and 6 mm diameter tubes, respectively. Table 2 is a listing of the results of these tests. The Doppler balloon catheter appeared to exhibit the most linear behavior in the larger tubes. A graph of the velocity expressed as a frequency shift in KHz, as measured by the Doppler balloon catheter, versus average velocity measured by timed collection for the 4 mm diameter tube is shown in Figure 5. This figure is typical of the larger tubes and demonstrates the linear relationship between the Doppler frequency and the velocity.

Pulsatile-flow model

The next phase of the experimental program was to test if the linearity of the Doppler balloon catheter was effected by movement of the catheter inside the lumen of the tube as a result of phasic changes in flow. The pulsatile-flow model used stainless steel tubes of 2, 3, 4, and 6 mm internal diameter with a port built into the

Table 2. Listing of velocities obtained in the steady-flow model by taking 10 random measurements with both the Doppler balloon catheter (DBC) and timed collection (velocity) in the 2, 3, 4, and 6 mm tubes

2 mm I.D.		3 mm I.D.		4 mm I.D.		6 mm I.D.	
DBC (KHz)	Velocity (cm/s)	DBC (KHz)	Velocity (cm/s)	DBC (KHz)	Velocity (cm/s)	DBC (KHz)	Velocity (cm/s)
0.00	0.0	0.00	0.0	0.06	0.0	0.10	0.0
0.02	6.7	0.08	10.0	1.14	13.3	1.08	14.8
0.04	12.1	0.14	17.3	2.00	23.0	1.74	22.1
0.06	23.9	0.18	21.1	3.44	35.6	2.20	33.5
0.08	31.5	0.26	25.2	3.90	47.0	2.88	51.7
0.10	36.9	0.36	36.2	5.20	55.1	3.50	63.7
0.12	38.2	0.46	45.3	6.16	67.7	4.40	72.2
0.14	43.9	0.54	47.0	7.30	79.7	5.46	95.4
		0.60	55.0	7.82	91.8	5.76	99.7
		0.66	58.3	8.44	101.9	5.94	104.8

Figure 5. Measurements of velocity in a 4 mm internal diameter tube with the Doppler balloon catheter in an in vitro steady-flow series

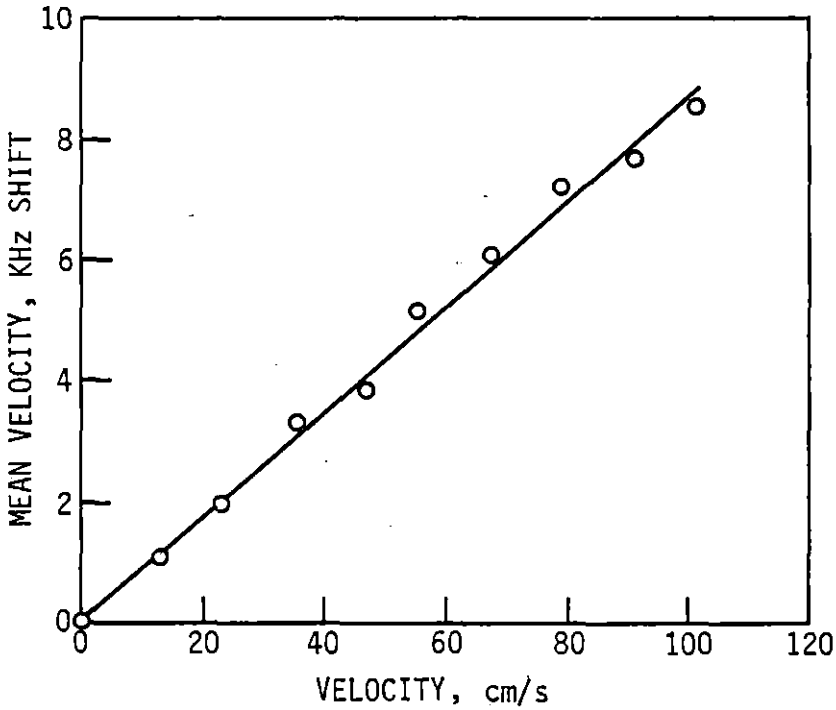
MEAN VELOCITY, KHz SHIFT
VELOCITY, cm/s
0
2
4
6
8
10
0
20
40
60
80
100
120

wall of the tube. A 20 MHz ultrasonic piezoelectric crystal was placed in the port at an approximately 45 degree angle pointing in the same direction as flow. The fixed Doppler crystal was used to identify any differences in the Doppler balloon catheter due to movement of the catheter. A Harvard pulsatile pump was used to generate the phasic flow pattern. An electromagnetic flowmeter, the Doppler crystal mounted in the port, and timed collection were used as standards. A diagram of the pulsatile-flow model is shown in Figure 6. The pump was turned on and off to compare the reaction of the three devices to transient changes in flow. All three devices appeared equally responsive to phasic changes in flow.

Pulsatile flow data were obtained at 4-5 random flow rates. Peak velocity ranged from 50 cm/s in the 2 mm tube to 90 cm/s in the 3, 4, and 6 mm tubes. Reynolds numbers ranged from 356-5552 and the Womersley (α) parameter varied from 1.08-7.96. Because of the pump and system used, only 4-5 random flows were generated. The Doppler balloon catheter yielded correlation coefficients for mean velocity of 0.856, 0.802, 0.973, and 0.999 for the 2, 3, 4, and 6 mm diameter tubes, respectively, when compared with mean velocities obtained by timed collections. Table 3 is a listing of the results of these tests. The Doppler balloon catheter was again most linear in the

Figure 6. Diagram of the pulsatile-flow system

PULSATILE-FLOW MODEL

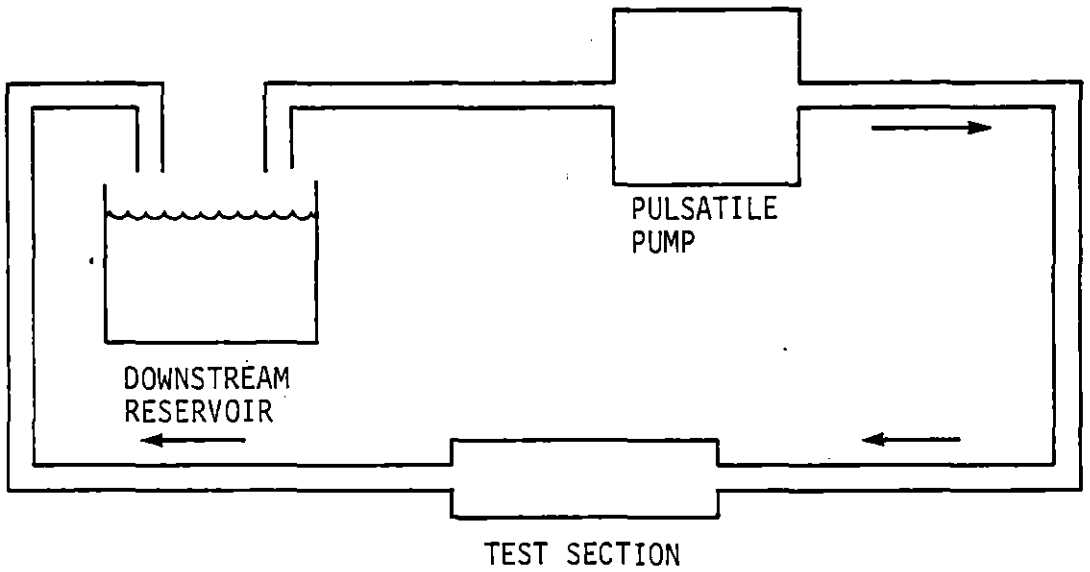

TEST SECTION

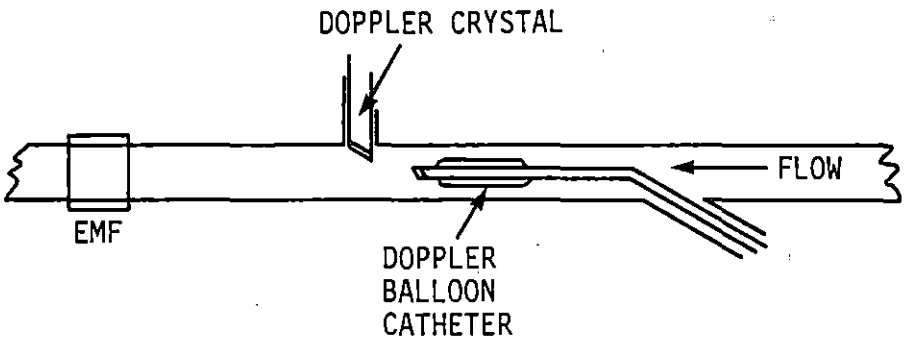

larger tubes. A typical graph of velocity measured by the Doppler balloon catheter in KHz versus mean velocity measured by timed collection for the 4 mm tube is shown in Figure 7. The Doppler balloon catheter yielded correlation coefficients for peak velocity compared to peak flow measured by the electromagnetic flowmeter of 0.917, 0.938, 0.982, and 0.999 for the 2, 3, 4, and 6 mm tubes, respectively. Table 4 is a listing of peak velocities obtained by this method. Figure 8 is a graph of peak velocity measured by both the Doppler balloon catheter and the fixed Doppler crystal in KHz versus flow measured by the electromagnetic flowmeter in volts. The straight lines shown in Figure 7 and Figure 8 are included to simply indicate the ideal response, i.e., a linear variation over a wide range of velocities. Deviation from these lines represent a combination of experimental scatter in the data and nonlinear behavior of the devices.

In Vivo Studies

In vivo testing consisted of catheterizing the arteries of 5, 20-25 Kg dogs in the same direction as flow in an approximately 3-5 mm internal diameter section. The dog femoral artery was chosen as an in vivo model of the human coronary circulation because it has similar diameters and flow rates without the added complication of

Table 3. Listing of mean velocities obtained in the pulstaile-flow model by taking 4-5 random measurements with the Doppler balloon catheter (DBC), fixed Doppler crystal (Crystal), electromagnetic flowmeter (EMF), and timed collection (Velocity) in the 2, 3, 4, and 6 mm tubes

	DBC (KHz)	Crystal (KHz)	EMF (Volts)	Velocity (cm/s)
2 mm I.D.	0.0	0.0	0.00	0.0
	4.5	2.6	0.02	15.9
	10.3	8.1	0.06	29.0
	10.2	6.7	0.05	42.3
3 mm I.D.	0.0	0.0	0.00	0.0
	2.6	5.0	0.04	16.5
	8.2	9.4	0.12	35.1
	22.9	13.0	0.05	49.0
	14.6	13.8	0.15	59.1
4 mm I.D.	0.0	0.0	0.00	0.0
	3.6	3.2	0.06	13.2
	7.1	5.4	0.12	25.7
	15.2	10.0	0.21	56.0
	18.4	13.6	0.38	90.2
6 mm I.D.	0.0	0.0	0.00	0.0
	1.5	1.6	0.07	7.4
	5.9	4.9	0.30	24.5
	11.7	9.4	0.54	49.0
	18.9	14.5	0.89	82.6

Figure 7. Measurements of velocity in a 4 mm internal diameter tube with the Doppler balloon catheter in an in vitro pulsatile-flow system

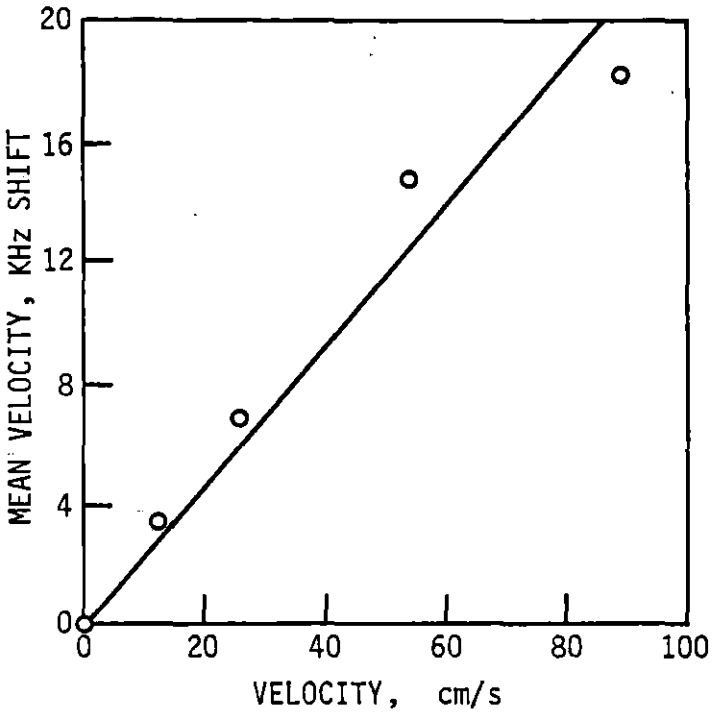
20
16
12
8
4
0
MEAN VELOCITY, KHz SHIFT
0
20
40
60
80
100
VELOCITY, cm/s

Table 4. Listing of peak velocities obtained in the pulsatile-flow model by taking 4-5 random measurements with the Doppler balloon cathether (DBC), fixed Doppler crystal (Crystal), and electromagnetic flowmeter (EMF) in the 2, 3, 4, and 6 mm tubes

	DBC (KHz)	Crystal (KHz)	EMF (Volts)
2 mm I.D.	0.00	0.00	0.00
	7.69	4.49	0.04
	9.76	10.13	0.04
	13.43	8.98	0.08
3 mm I.D.	0.00	0.00	0.00
	5.43	10.08	0.09
	13.10	14.33	0.20
	17.52	17.87	0.20
	16.73	17.01	0.20
4 mm I.D.	0.00	0.00	0.00
	7.44	6.26	0.12
	15.39	10.91	0.26
	25.35	18.23	0.49
	29.41	22.17	0.70
6 mm I.D.	0.00	0.00	0.00
	2.99	3.15	0.18
	13.58	10.39	0.59
	25.24	19.96	1.21
	36.73	25.71	1.86

Figure 8. Graph of peak velocity measured by both the Doppler balloon catheter and the fixed Doppler crystal in KHz versus peak velocity measured by the electromagnetic flowmeter (EMF) in volts in the 4 mm tube

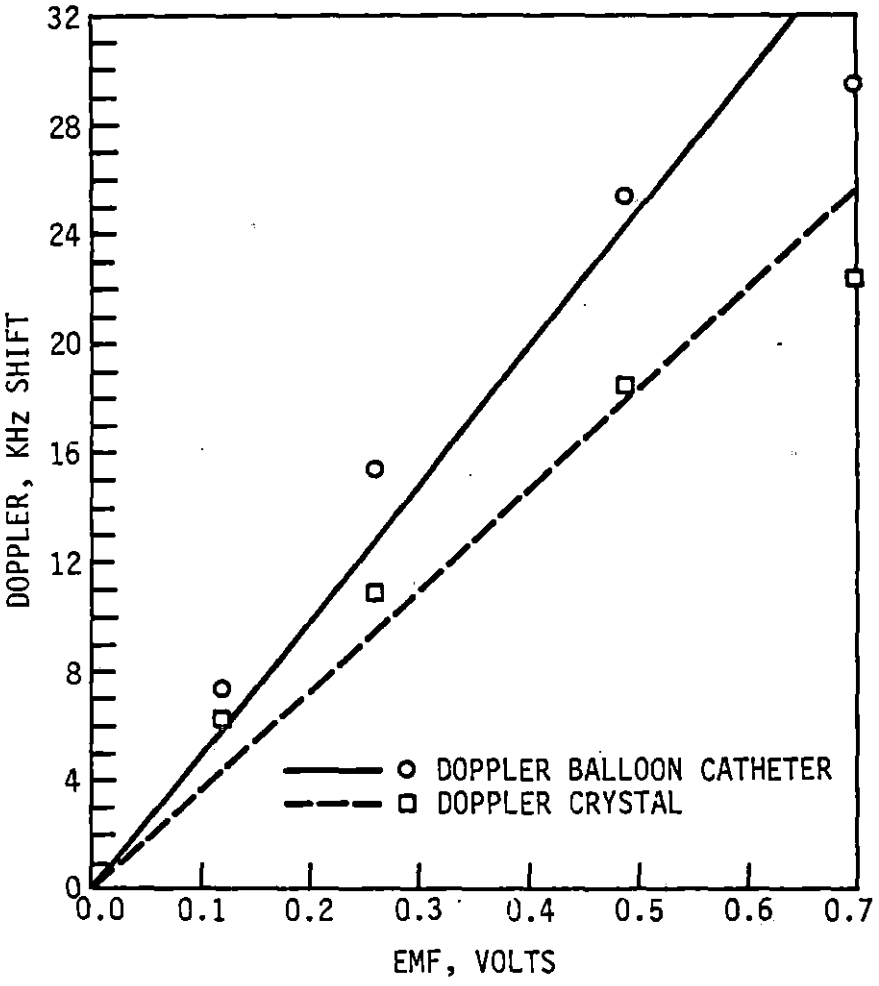
32
28
24
20
16
12
8
4
0
DOPPLER, KHz SHIFT
0.0
0.1
0.2
0.3
0.4
0.5
0.6
0.7
EMF, VOLTS
DOPPLER BALLOON CATHETER
DOPPLER CRYSTAL

movement due to the contraction of the heart as exists in the coronary circulation. The standard used to evaluate the ability of the Doppler balloon catheter to measure phasic velocity and reactive hyperemia was the suction Doppler probe developed by Marcus et al. (1981).

In the first experiments, the Doppler balloon catheter was entered into the abdominal aorta in the direction of the femoral artery. Though measurements in the femoral artery were attempted, none proved successful. Thus, the first two experiments, data collection was limited to placement of the catheter in the lower abdominal aorta and iliac artery, and no simultaneous measurements (balloon catheter and suction Doppler) were obtained. Temporary occlusions were generated by clamping the abdominal aorta for 20-30 seconds.

For the last three experiments, the surgical procedure was changed. In order to facilitate catheterization, the Doppler balloon catheter was entered into the left external carotid and guided with fluoroscopy into the left femoral artery. The femoral artery was exposed so that the suction Doppler probe could be placed distal to the tip of the Doppler balloon catheter. Arterial pressure was recorded by placing a cannula in the right femoral artery. Phasic velocity and reactive hyperemia were monitored. Some simultaneous recordings of phasic velocity and reactive

hyperemia were recorded in two of the experiments. Samples of some of the best recordings follow. These particular recordings were taken with the Doppler balloon catheter placed in the caudal iliac - cranial femoral artery. Temporary 20-30 sec occlusions were generated by occluding the femoral artery distal to the tip of the Doppler balloon catheter. Figure 9 is a recording of phasic velocity with the Doppler balloon catheter and arterial pressure in the femoral artery of an anesthetized dog. A recording of reactive hyperemia as determined with the Doppler balloon catheter, and arterial pressure following a 20 sec femoral occlusion is shown in Figure 10. Figure 11 shows a simultaneous recording of phasic velocity by both the Doppler balloon catheter and the suction Doppler probe. A simultaneous recording of reactive hyperemia following a 20 sec femoral occlusion is shown in Figure 12. Although the balloon of the Doppler balloon catheter has been used to generate temporary occlusions to flow, the proceeding recordings used occlusions where the femoral artery was clamped shut because the catheter was located in a greater than 3 mm internal diameter section of the vessel.

These dog studies demonstrated the ability of the Doppler balloon catheter to measure phasic velocity and reactive hyperemia in a 3-5 mm internal diameter section of artery. Furthermore, the phasic velocity and the reactive

Figure 9. Recording of phasic velocity with the Doppler balloon catheter and arterial pressure in the femoral artery of an anesthetized dog

Figure 10. Recording of mean velocity with the Doppler balloon catheter and arterial pressure following transient femoral artery occlusion in an anesthetized dog

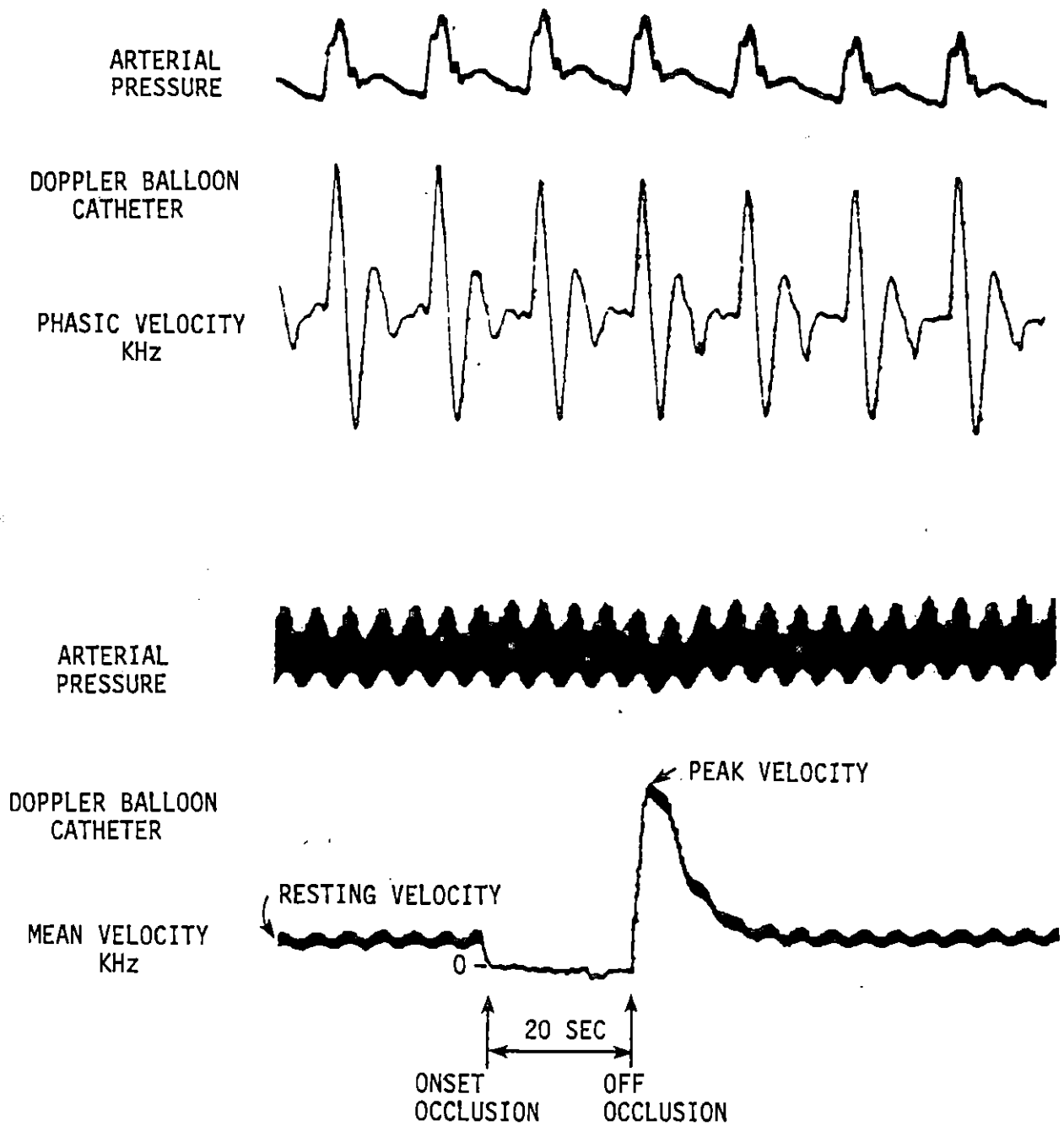
ARTERIAL PRESSURE
DOPPLER BALLOON CATHETER
PHASIC VELOCITY KHz
ARTERIAL PRESSURE
DOPPLER BALLOON CATHETER
MEAN VELOCITY KHz
PEAK VELOCITY
RESTING VELOCITY
0
20 SEC
ONSET OCCLUSION
OFF OCCLUSION

Figure 11. Simultaneous recordings of phasic velocity by both the Doppler balloon catheter and the suction Doppler probe on the femoral artery of an anesthetized dog

Figure 12. Simultaneous recordings of mean velocity with the Doppler balloon catheter and suction Doppler probe following transient femoral artery occlusion in an anesthetized dog

DOPPLER BALLOON CATHETER

PHASIC VELOCITY KHz

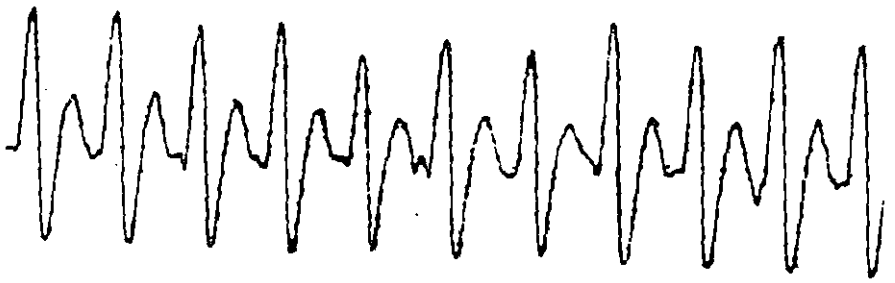

SUCTION DOPPLER PROBE

PHASIC VELOCITY KHz

DOPPLER BALLOON CATHETER

MEAN VELOCITY KHz

SUCTION DOPPLER PROBE

MEAN VELOCITY KHz

hyperemic response measured by the Doppler balloon catheter was similar to that obtained with the extraluminal suction Doppler probe.

DISCUSSION OF EXPERIMENTS

The in vitro and in vivo models of the coronary circulation used in this study have demonstrated the approximate linearity of the device and its ability to measure phasic velocity and reactive hyperemia. Although the linearity of the Doppler balloon catheter was in general less in the pulsatile-flow model (compared to the steady-flow model), the capability of the device to measure phasic velocity and reactive hyperemia was similar to that measured by the extraluminal suction Doppler probe. The Doppler balloon catheter appeared to perform best in vessels and tubes greater than 3 mm and less than 6 mm in diameter.

A problem with the Doppler balloon catheter prototype appears to be the fact that at vessel diameters of 3 mm and less, the catheter became almost incapable of recording meaningful data with either mean or phasic flow. Another inherent problem with the intraluminal Doppler balloon catheter is that the exact position of the Doppler crystal relative to the center of the vessel is difficult to control.

HEMODYNAMIC EVALUATION AND DEVELOPMENT OF THEORETICAL MODEL

A separate aspect of the study was to determine what effect the placement of a catheter in an artery might have upon mean velocity and reactive hyperemia. In the normal artery, the major contributor of resistance to flow is made by the peripheral vascular beds. This resistance is called the peripheral resistance. The effect of a stenosis is to generate a second resistance which will be referred to as stenosis resistance. The presence of the catheter within the vessel will add an additional resistance to the system, and the total resistance to flow within a catheterized, obstructed vessel is then the sum of these three resistances.

When the vessel is temporarily occluded during measurements of reactive hyperemia, the peripheral resistance falls to a minimum value. The subsequent increase in flow after release of occlusion is governed only by whatever resistance remains. In the case of an obstructed artery, the peak flow after release of occlusion varies inversely with the severity of the stenosis. The addition of the catheter to the system adds an additional resistance to the system which further decreases the peak flow after release of occlusion. Therefore, to evaluate the signifi-

cance of stenosis resistance upon the mean peak to resting flow ratio, the contribution due to catheter resistance must be considered.

Idealized Model

In order to estimate the hemodynamic effect of the catheter, a highly simplified model has been developed. The model assumes the catheter to be inserted concentrically within an unobstructed vessel of constant diameter and neglects the effect of the balloon. In addition, steady flow is assumed. A diagram of the model is shown in Figure 13. The model considers the pressure drop at various points as the ratio, r_1/r_0 (where r_1 is the catheter radius and r_0 is the vessel radius), and the dimensionless axial distance from the entrance of the vessel, ℓ/r_0, is varied. The model assumes vessels of constant diameter with steady flow, Q, at constant Reynolds numbers, Re.

The flow rates and vessel diameter chosen for the model are based on values for internal diameter and mean resting and mean hyperemic flow rates commonly found in the coronary circulation. Gould et al. (1974) determined that the left circumflex coronary artery of dogs has an average outside diameter of 3.3 ± 0.3 mm (S.D.), mean resting flow of 48 ± 18 ml/min (S.D.) and a

Figure 13. Diagram of the catheter hemodynamic model

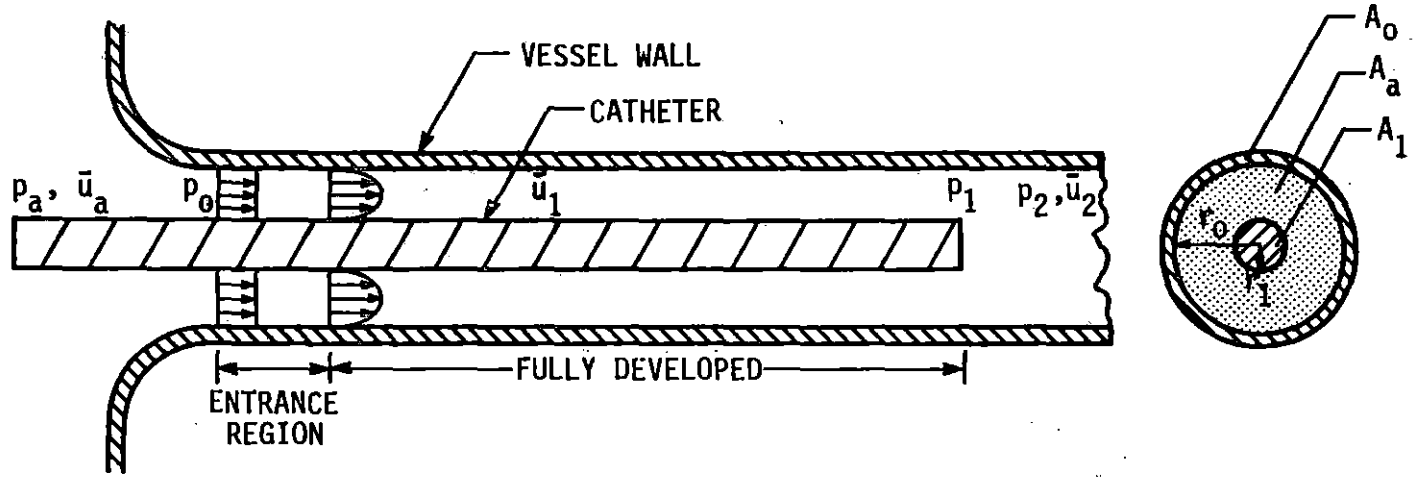
VESSEL WALL
CATHETER
p_a, $\bar{u}_a$
p_0
$\bar{u}_1$
p_1
p_2, $\bar{u}_2$
ENTRANCE REGION
FULLY DEVELOPED
A_o
A_a
A_1
r_o
r_1

mean peak to resting flow ratio of 4.3 $\pm$ 0.9 (S.D.). Kirkeeide (1978) found in the left circumflex artery of dogs an average lumen diameter of 3.0 mm, mean resting flow of 40 $\pm$ 14 ml/min (S.D.), and an average mean peak to resting flow ratio of 4.8. Marcus et al. (1981) found a peak to mean resting flow ratio of 5.8 $\pm$ 0.6 (S.D.) in the coronary circulation of humans. Based on these references, it was decided to use a model lumen diameter of 3.0 mm, mean resting velocity of 10 cm/s, and a mean peak to resting flow ratio of 5.0. The initial pressure and velocity at the coronary artery entrance is taken as that of the ascending aorta. Milnor (1982) lists a value for human ascending aorta mean velocity, $\bar{u}_a$, of 16 cm/s and ascending aorta mean pressure, p_a, as 85 mm Hg. Milnor also lists blood density, ρ, as 1050 Kg/m3 and blood viscosity, μ, of 0.004 N.s/m2.

To simulate coronary catheterization, catheter sizes of 2, 3, 4, and 5 Fr were used. Table 5 shows the diameter, D_1, and r_1/r_0 ratio for each catheter size. The axial distances, ℓ, from the entrance of the vessel to the distal tip of the catheter used in the model were 2, 4, 6, 8, and 10 cm. To evaluate the pressure drop at mean hyperemic flow, a velocity of 5 times resting velocity was used. Thus, pressure drops were calculated at a resting velocity of 10 cm/s (Q = 42.4 ml/min, Re = 79)

Table 5. Table of catheter diameter and catheter to vessel radius ratio for each catheter size (D_0=3. mm)

Catheter size	D_1 mm	r_1/r_0
2 Fr	0.67	0.22
3 Fr	1.00	0.33
4 Fr	1.33	0.44
5 Fr	1.67	0.56

and a hyperemic velocity of 50 cm/s (Q = 212.0 ml/min, Re = 395).

Calculations

Five sets of calculations were performed in conjunction with the model. The first step utilized the Bernoulli equation to estimate the pressure drop, $\Delta p = p_a - p_0$, between the ascending aorta and the entrance region of the coronary artery. With the mean velocity of the ascending aorta, $\bar{u}_a$, mean velocity of the coronary artery, $\bar{u}_0$, and blood density, ρ, known, the pressure drop, $\Delta p = p_a - p_0$, could be calculated through the equation

$$p_a + \frac{1}{2}(\rho \bar{u}_a^2) = p_0 + \frac{1}{2}(\rho \bar{u}_0^2) \qquad (1)$$

The pressure drop was calculated at both resting and hyperemic velocities. In both cases, the value for the pressure drop was less than 1 mm Hg. Therefore, it was assumed that the mean pressure in the entrance region of the vessel was approximately equal to the mean pressure of the ascending aorta ($p_0 \simeq p_a = 85$ mm Hg).

Next, the pressure drop, $\Delta p = p_0 - p_1$, from the entrance of the vessel to some axial distance from the entrance of the vessel without a catheter was calculated. The axial distances from the entrance considered were 2, 4, 6, 8, and 10 cm. The pressure drops at both resting and hyperemic conditions were calculated for each axial distance. The method developed by Schmidt and Zeldin (1969) was used. This particular method was chosen because it allows evaluation of the velocity distribution and pressure drop with laminar flows in inlet sections of tubes. The axial distance from the entrance, vessel diameter, and Reynolds number must be known to evaluate the pressure drop. The pressure drop at various axial distances from the entrance of the vessel can be obtained from the equation

$$\frac{p_0 - p_1}{\frac{1}{2}(\rho \bar{u}_0^2)} = fZ + K \qquad (2)$$

where f is the fully developed friction factor

$$f = 64/Re$$

with

$$Re = \frac{\rho \bar{u}_0 D_0}{\mu}$$

and Z is the nondimensional axial distance from the vessel entrance

$$Z = \ell/D_0$$

where D_0 is the diameter of the vessel.

The entrance region pressure drop coefficient, K, is a function of axial position and reaches an asymptotic value as the flow becomes fully developed. In order to determine K, a graph developed by Schmidt and Zeldin of K versus Z/Re for varying Reynolds numbers was used. With Re and Z/Re known, K could be estimated. With f, Z, K, ρ, and $\bar{u}_0$ specified, the pressure drop, $\Delta p = p_0 - p_1$, could be determined. Table 6 is a listing of the pressure drop divided by mean ascending aorta pressure, $\Delta p/p_a$, calculated for the resting and hyperemic condition for each axial distance from the tube entrance.

The next step was to calculate the pressure drop created by 2, 3, 4, and 5 Fr catheters. The pressure drop at both resting and hyperemic conditions was calculated for axial distances from the entrance of the vessel of 2, 4, 6, 8, and 10 cm. The relationships developed

Table 6. Table of dimensionless pressure drop with no catheter

ℓ/r_0	Resting $\Delta p/p_a$	Hyperemic $\Delta p/p_a$
13.33	0.003	0.024
26.67	0.006	0.038
40.08	0.008	0.052
53.33	0.011	0.065
66.67	0.013	0.077

by Sparrow and Lin (1964) were used for these calculations. In this study, Sparrow and Lin developed an analytical method for determining the laminar flow and pressure drop in the entrance region of annular ducts. This method lends itself well to the present study if the catheter is assumed to be positioned concentrically within a vessel of constant diameter and constant Reynolds number. This method is based on an equation similar to that used in the previous set of calculations, i.e.,

$$\frac{P_0-P_1}{\frac{1}{2}(\rho\bar{u}_1^2)} = f\frac{\ell}{D_h} + K \qquad (3)$$

where D_h is the hydraulic diameter,

$$D_h = 2(r_0-r_1)$$

$\bar{u}_1$ is the mean annular velocity,

$$\bar{u}_1 = \frac{Q}{(A_0-A_1)} = \frac{\bar{u}_0 r_0^2}{(r_0^2-r_1^2)}$$

and Re is given by the relationship

$$Re = \frac{\rho \bar{u}_1 D_h}{\mu}$$

The friction factor, f, is calculated from the equation

$$f \cdot Re = \frac{64(1-(r_1/r_0))^2}{(1+(r_1/r_0)^2) - \frac{(1-(r_1/r_0)^2)}{\ln(r_0/r_1)}} \qquad (4)$$

The value of K was determined from a graph developed by Sparrow and Lin in which K versus 4(Z/Re) is given for various values of r_1/r_0. Table 7 gives the pressure drop divided by mean ascending aorta pressure, $\Delta p/p_a$, at resting and hyperemic conditions for each of the axial distances from the entrance of the vessel.

The next step was to estimate the pressure rise, $\Delta p = p_1-p_2$, in the expansion region just distal to the tip of the catheter. The momentum equation was used to evaluate the system. The derivation of pressure drop utilizing the momentum equation is given in the Appendix. For the range of parameters considered in this study, the pressure rise was found to be negligible. Thus, for all

Table 7. Table of dimensionless pressure drop for each catheter size and axial distance from the entrance of the vessel

Catheter size ℓ/r_0	2 Fr $\Delta p/p_a$	3 Fr $\Delta p/p_a$	4 Fr $\Delta p/p_a$	5 Fr $\Delta p/p_a$
A. Resting flow conditions				
13.33	0.007	0.010	0.015	0.029
26.67	0.013	0.019	0.029	0.058
40.00	0.019	0.028	0.044	0.087
53.33	0.026	0.038	0.058	0.115
66.67	0.032	0.047	0.073	0.144
B. Hyperemic flow conditions				
13.33	0.041	0.057	0.084	0.160
26.67	0.074	0.104	0.157	0.305
40.00	0.106	0.151	0.229	0.449
53.33	0.138	0.198	0.301	0.593
66.67	0.170	0.245	0.373	0.737

practical purposes, the significant pressure gradient induced by the catheter is $\Delta p = p_0 - p_1$, i.e., entrance and exit effects are very small compared to the pressure drop in the annular region along the catheter. Graphs of $(p_0-p_1)/p_a$ versus ℓ/r_0 for both resting and hyperemic flow rates were constructed for each of the 2, 3, 4, and 5 Fr catheters. These dimensionless graphs are shown in Figures 14, 15, 16 and 17, respectively.

Figure 14. A graph of dimensionless pressure drop versus dimensionless axial distance for the 2 Fr catheter

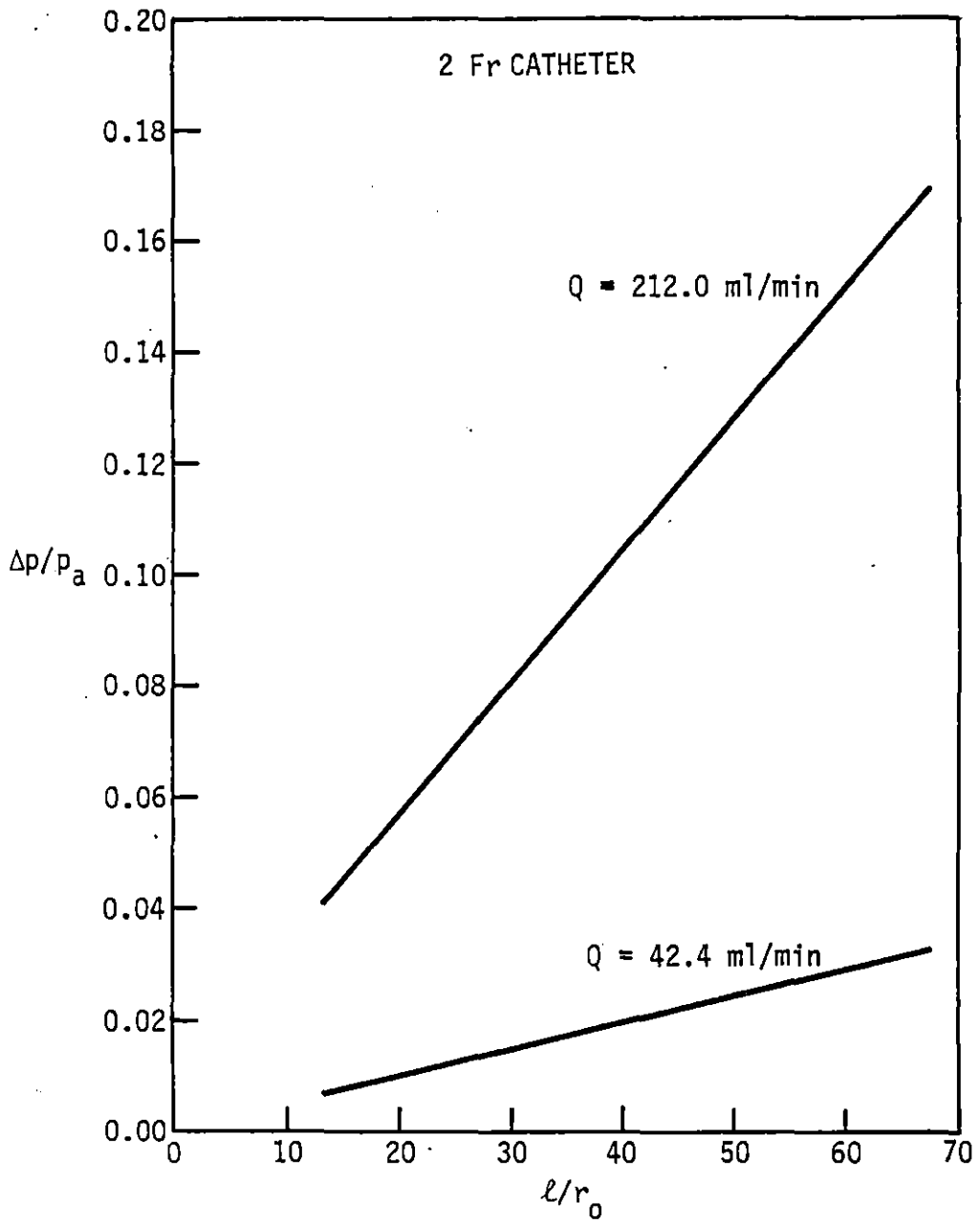
2 Fr CATHETER
Q = 212.0 ml/min
Q = 42.4 ml/min
Δp/p_a
0.20
0.18
0.16
0.14
0.12
0.10
0.08
0.06
0.04
0.02
0.00
0
10
20
30
40
50
60
70
ℓ/r_o

Figure 15. A graph of dimensionless pressure drop versus dimensionless axial distance for the 3 Fr catheter

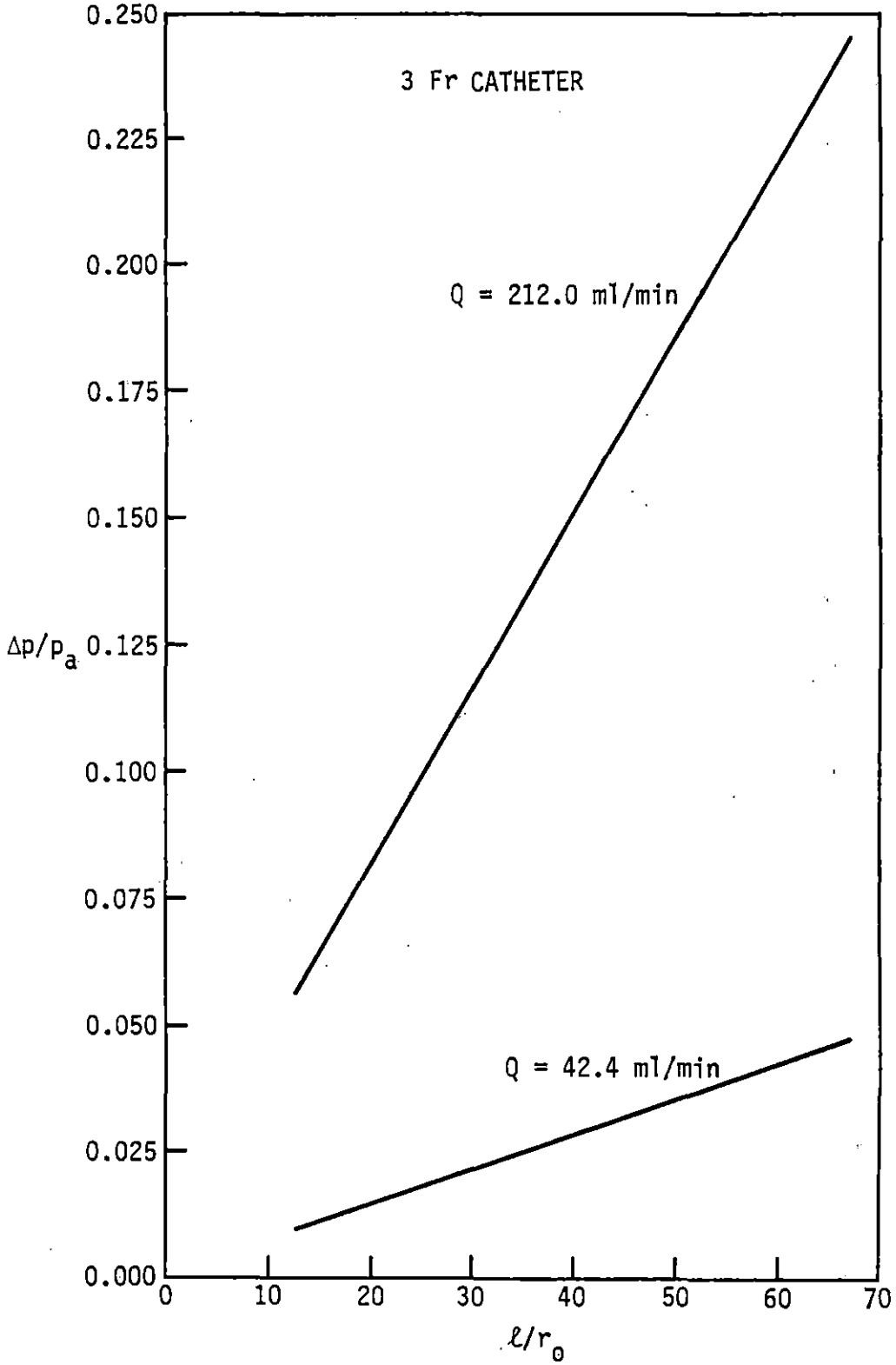
3 Fr CATHETER
Q = 212.0 ml/min
Q = 42.4 ml/min
0.250
0.225
0.200
0.175
0.150
0.125
0.100
0.075
0.050
0.025
0.000
Δp/p_a
0
10
20
30
40
50
60
70
ℓ/r_0

Figure 16. A graph of dimensionless pressure drop versus dimensionless axial distance for the 4 Fr catheter

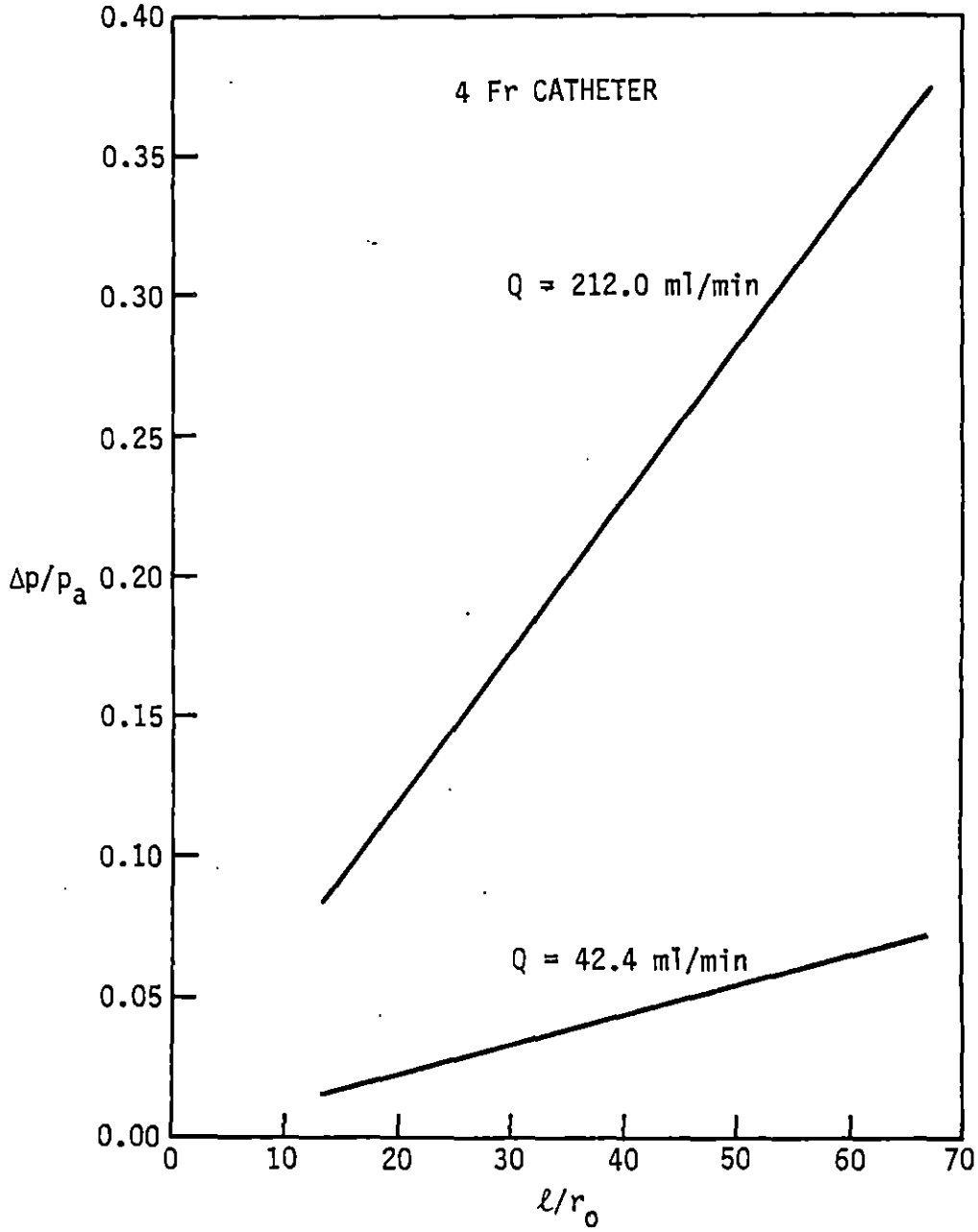
4 Fr CATHETER
Q = 212.0 ml/min
Q = 42.4 ml/min
Δp/p_a
0.40
0.35
0.30
0.25
0.20
0.15
0.10
0.05
0.00
0
10
20
30
40
50
60
70
ℓ/r_o

Figure 17. A graph of dimensionless pressure drop versus dimensionless axial distance for the 5 Fr catheter

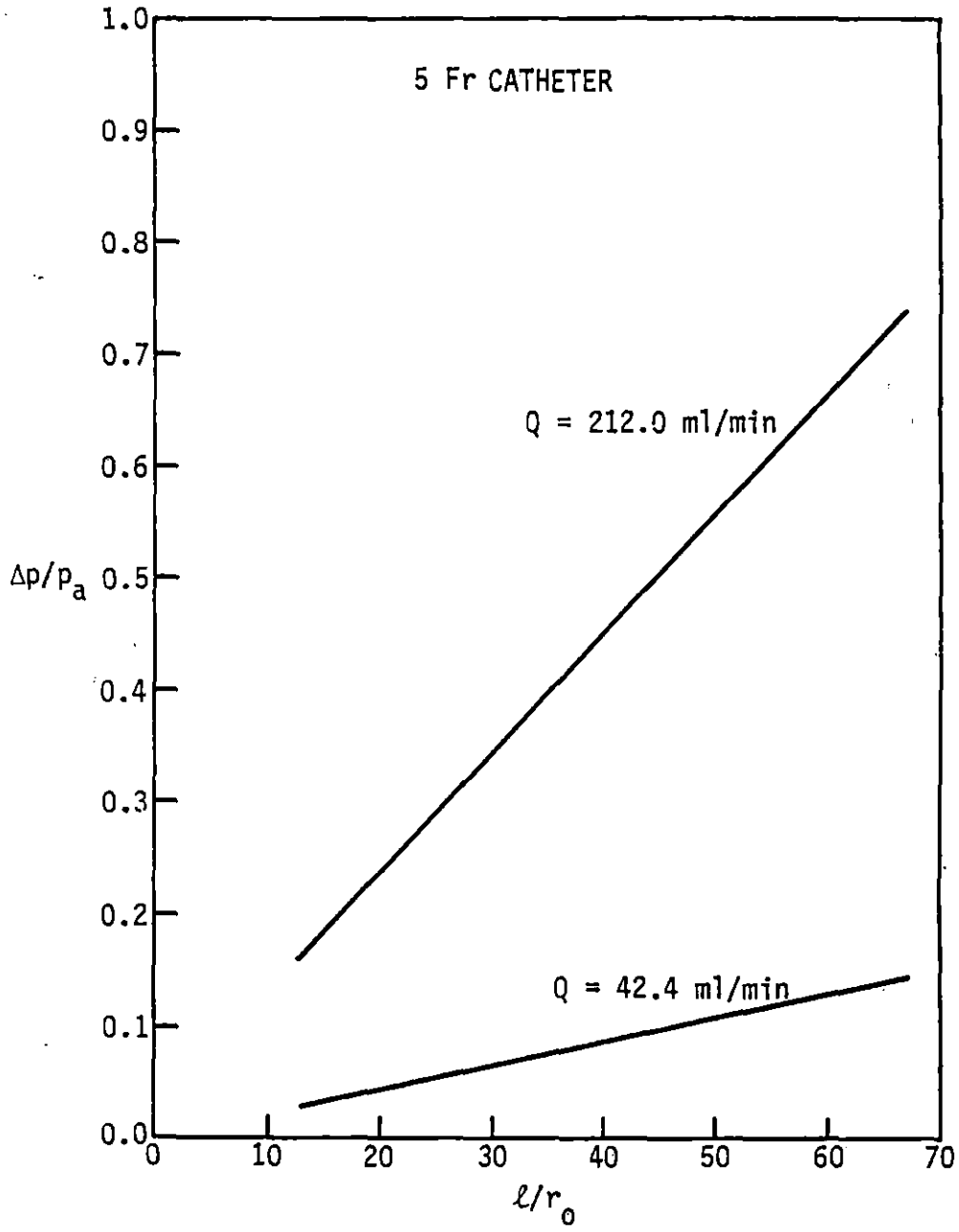
5 Fr CATHETER
Q = 212.0 ml/min
Q = 42.4 ml/min
Δp/p_a
ℓ/r_o
1.0
0.9
0.8
0.7
0.6
0.5
0.4
0.3
0.2
0.1
0.0
0
10
20
30
40
50
60
70

Stenosis Equivalent of Catheter

In order to have a better appreciation of the effects of the pressure drop induced by the catheter, pressure drops where converted to equivalent percent stenosis through the use of an equation developed by Young et al. (1977) relating the pressure drop induced by a stenosis to various factors. The stenosis equation is

$$\Delta P = P_1 - P_2 = K_v \frac{\mu \bar{U}_0}{d_0} + \frac{K_t}{2} ((a_0/a_1)-1)^2 \rho \bar{U}_0^2 \qquad (5)$$

where:

$$K_v = 32 \frac{\ell_a}{d_0} (a_0/a_1)^2$$

$$\ell_a = 0.83\ \ell_s + 1.64\ d_1$$

$$\ell_s = 2d_0$$

$$d_1 = 2\left[\frac{D_0/2}{(a_0-a_1)}\right]^{1/2}$$

$$Kt = 1.5$$

for the blunt plug stenosis shown in Figure 18. Values of pressure drop across the stenosis were calculated at resting and hyperemic conditions for various percent stenosis, where percent stenosis is defined as

$$\text{Percent Stenosis} = (1-(a_1/a_0))100$$

Figure 18. A diagram of the stenosis hemodynamic model

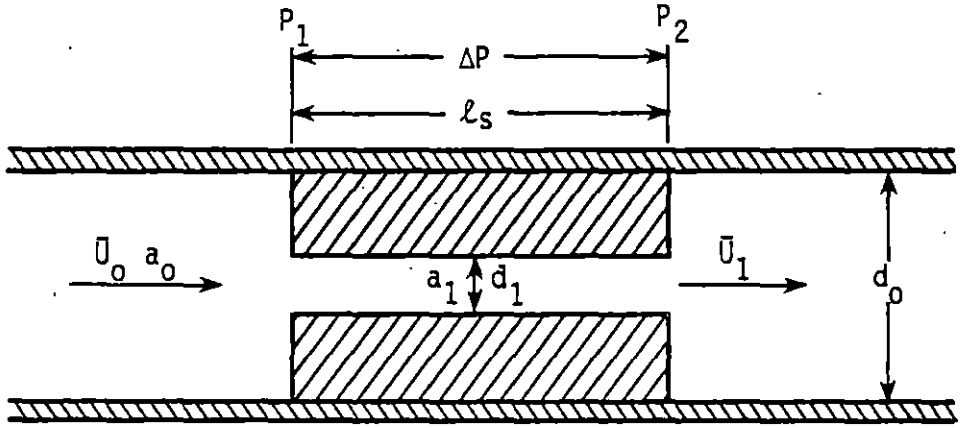
P1
P2
ΔP
ℓs
Ū0 a0
a1
d1
Ū1
d0

Figure 19 is a graph of $\Delta P/p_a$ versus percent stenosis for both the resting and hyperemic conditions. With this information, the dimensionless pressure drop, $\Delta p/p_a$, for each catheter size and axial distance from the entrance can be compared with these results to obtain an equivalent stenosis.

Figure 19. Graph of dimensionless pressure drop versus percent stenosis for both the resting and hyperemic conditions for a blunt plug stenosis with $\ell_s/d_0 = 2$

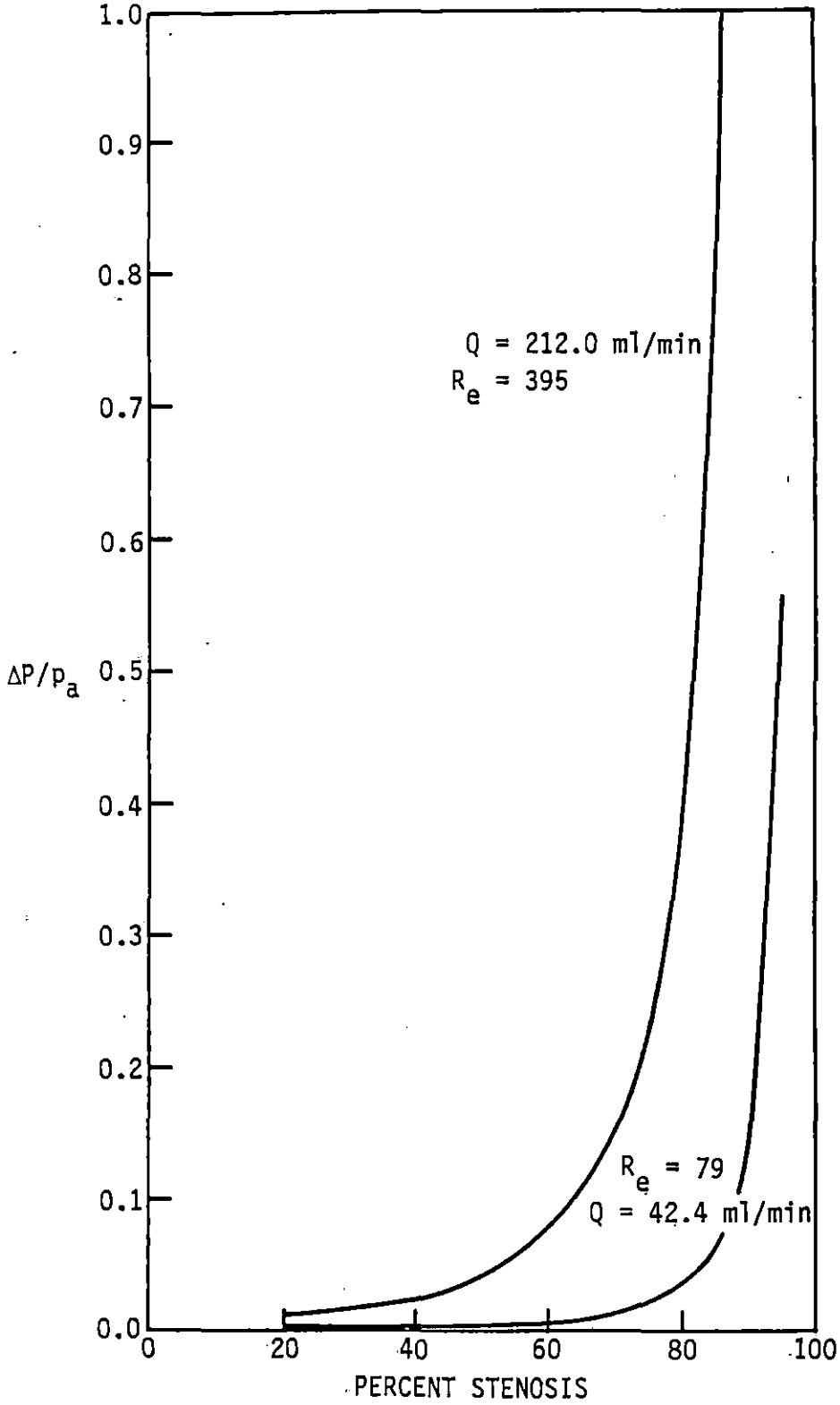
1.0
0.9
0.8
0.7
0.6
0.5
0.4
0.3
0.2
0.1
0.0
ΔP/p_a
Q = 212.0 ml/min
R_e = 395
R_e = 79
Q = 42.4 ml/min
0
20
40
60
80
100
PERCENT STENOSIS

DISCUSSION OF THEORETICAL MODEL RESULTS

The major contribution to the pressure gradient created by the catheter has been shown to be in the section from p_0 to p_1, i.e., where $p_a - p_2 \simeq p_0 - p_1$. This pressure drop increases with increases in flow rate and axial distance from the entrance and can be significant. For example, a 4 Fr catheter in a 3 mm vessel at ℓ = 10 cm produces a pressure drop equivalent to an 86 percent stenosis in the resting flow case and an 80 percent stenosis at the hyperemic flow rate. The fact that an 85 percent stenosis is generally considered critical and the fact that a stenosis becomes critical sooner at elevated flow rates, casts doubt on the ability of a 4 Fr Doppler balloon catheter to assess the significance of an obstruction in a 3 mm internal diameter section of coronary artery located 10 cm distal to the coronary ostia. Because of the exponential behavior of $\Delta P/p_a$ versus percent stenosis (Figure 19), $\Delta P/p_a$ drops abruptly at values less than 80-85 percent stenosis. It is therefore indicated by this model that the Doppler balloon catheter should be at least less than 4 Fr in order to assess coronary obstructions in arterial segments having diameters of 3 mm or less, and ℓ = 10 cm. It should be emphasized that decreasing ℓ or Q, or in-

creasing D_0 would decrease $\Delta p/p_a$, allowing a larger diameter catheter to be used.

SUMMARY AND CONCLUSIONS

Data collected from this study suggest that it may be possible to assess the significance of coronary obstructions using the Doppler balloon catheter method. The in vitro and in vivo models have demonstrated the approximate linearity of the device, and its ability to measure phasic velocity and reactive hyperemia. Although the linearity of the Doppler balloon catheter was in general less in the pulsatile-flow model (compared to the steady-flow model), the capability of the device to measure phasic velocity and reactive hyperemia was similar to that measured by the extraluminal suction Doppler probe. The Doppler balloon catheter appeared to perform best in tubes or vessels of greater than 3 mm internal diameter.

The idealized mathematical model revealed that a catheter to vessel radius ratio of about 0.44 and ℓ = 10 cm could produce a pressure drop equivalent to that induced by a critical stenosis. This means that the catheter to vessel radius ratios should be at least less than 0.44 in order to attempt measurements of the significance of coronary arterial obstructive lesions. The 4 Fr Doppler balloon catheter prototype seemed to work best in vessels and tubes of 4 mm internal diameter. This equates to a catheter to vessel radius ratio of 0.33. This

ratio is equivalent to a 3 Fr catheter in a 3 mm internal diameter vessel. It should be noted that the catheter induced pressure gradient is a function of not only the relative size of the catheter but also the axial distance and flow rate. Thus, each case would have to be considered individually. Specific values used in the present study are simply intended to be representative of values commonly found in the coronary circulation.

Though precise quantitative estimates of percent stenosis by the Doppler balloon catheter appear to exceed the capability of the method, it may be possible, with more refinement of the prototype, to distinguish between critical and subcritical obstructions. It is hoped that the Doppler balloon method will eventually provide a method whereby the physiological significance of coronary obstructive lesions can be accurately assessed at the time of cardiac catheterization.

RECOMMENDATIONS FOR FURTHER STUDY

Future studies should be directed at scaling down the diameter of the Doppler balloon catheter. This is most important if evaluation of coronary obstructions remains the major goal of this research. The development of a 3 Fr or less size Doppler balloon catheter containing a minimum of an air lumen for the balloon and a lumen for electrical wires would be advantageous to the study. Such a catheter must be stiff enough to allow sufficient manipulation and directive ability.

In addition, better results might be elicited by a different placement of the Doppler crystal. A new design, in which the Doppler crystal is placed 2-3 cm proximal to the distal tip of the catheter pointed against flow, is currently being investigated by researchers at the University of Iowa. Rotation of the catheter, with this design, allows a better possibility to direct the crystal into the main flow stream and away from the wall. Preliminary results with this design have proved promising. It appears that the 4 Fr angioplasty catheter is too large in diameter for this application. A 3 Fr balloon catheter with a piezoelectric crystal mounted on the side pointed against flow would be a good choice for the next prototype. The distal balloon need only be capable of

temporarily occluding flow.

If these improvements can be accomplished, a more thorough investigation of the fluid mechanics of the system will be required. A more advanced mathematical pulsatile-flow model that takes into account the distal balloon, and the position and orientation of the catheter inside the vessel will probably show the pressure drops calculated by the present catheter hemodynamic model to be conservative. An improved model could be used to evaluate the total pressure drop in a vessel containing not only the catheter but a stenosis of varying severity at different flow rates. This would be followed by in vitro and in vivo modeling in order to confirm the results of the mathematical model. If the exact pressure drop could be accurately determined for a given catheter to vessel radius ratio, axial distance from the entrance of the vessel, and resting velocity, then it may be possible to separate the catheters contribution from the total pressure drop created by the catheter and stenosis. The only pressure drop remaining would be due to the stenosis. An accurate critical versus subcritical evaluation of the stenosis might then be possible.

LITERATURE CITED

Benchimol, A., H. F. Stegall, and J. L. Gartlan. 1971. New method to measure phasic coronary velocity in man. Am. Heart J. 81:93-101.

Bittar, N., G. M. Kroncke, G. C. Dacumos, Jr., G. C. Rowe, W. P. Young, P. S. Chopra, J. D. Folts, and D. R. Kahn. 1972. Vein graft flow and reactive hyperemia in the human heart. J. Thorac. Cardiovasc. Surg. 64:855-860.

Brown, B. G., E. Bolson, and M. Frimer. 1977. Quantitative coronary arteriography: estimation of dimensions, hemodynamic resistance, and atheroma mass of coronary artery lesions using the ateriogram and digital computation. Circulation 55(2):329-37.

Cole, J. S., and C. J. Hartley. 1977. The pulsed Doppler coronary artery catheter. Preliminary report of a new technique for measuring rapid changes in coronary artery flow velocity in man. Circulation 56:18-25.

Folts, J. D., G. G. Rowe, D. R. Kahn, and W. P. Young. 1979. Phasic changes in human right coronary blood flow before and after repair of aortic insufficiency. Am. Heart J. 97:211-215.

Gould, K. L., K. Lipscomb, and G. W. Hamilton. 1974. Physiologic basis for assessing critical coronary stenosis. Am. J. of Card. 33:87-94.

Greenfield, J. C., Jr., J. C. Rembert, W. G. Young, Jr., N. H. Oldham, Jr., J. A. Alexander, and D. C. Sabiston, Jr. 1972. Studies of blood flow in aorta-to-coronary venous bypass grafts in man. J. Clin. Invest. 51: 2724-2735.

Harrison, D. G., C. W. White, L. F. Hiratzka, C. B. Wright, D. B. Doty, M. R. Miller, C. L. Eastham, and J. L. Marcus. 1981. Can the significance of a coronary stenosis be predicted by quantitative coronary anglography? Circulation 64, Suppl. 4:160.

Hartley, C. J., H. G. Hanley, R. M. Lewis, and J. S. Cole. 1974. An ultrasonic pulsed Doppler system for measuring blood in small vessels. J. Appl. Physiol. 37: 626-629.

Hartley, C. J., H. G. Hanley, R. M. Lewis, and J. S. Cole. 1978. Synchronized pulsed Doppler blood flow and ultrasonic dimensional measurement in conscious dogs. Ultrasound Med. Biol. 4:99-110.

Kirkeeide, R. L. 1978. Mechanics of blood flow through normal and stenotic coronary arteries. Ph.D. Thesis. Iowa State University, Ames, Iowa.

Marcus, M., C. Wright, D. Doty, C. Eastham, D. Laughlin, P. Krumm, C. Fastenow, and M. Brody. 1981. A method for assessing the physiologic significance of coronary obstructions in man at cardiac surgery. Circulation 62:111-115.

Matthews, H. R., D. B. Skinner, and B. Pitt. 1971. Reactive hyperemia following coronary occlusion as a measurement of myocardial viability. Curr. Top. Surg. Res. 3:39-48.

Milnor, W. R. 1982. Hemodynamics. Williams and Wilkins. Baltimore, Maryland.

Olinger, G. N., D. G. Mulder, J. V. Maloney, and G. D. Buckberg. 1976. Phasic coronary flow: Intraoperative evaluation of flow distribution, myocardial function, and reactive hyperemia. Ann. Thorac. Surg. 21:397-404.

Schmidt, F. W., and B. Zeldin. 1969. Laminar flow in inlet sections of tubes and ducts. A.I.Ch.E. J. 15: 612-614.

Sparrow, E. m., and S. H. Lin. 1964. The developing laminar flow and pressure drop in the entrance region of annular ducts. J. Basic Engr. 86:827-834.

White, C., C. Wright, J. Furda, D. Doty, C. Eastham, D. Laughlin, and M. Marcus. 1980. Inability of the coronary arteriogram to predict the physiological significance of coronary stenosis. Clin. Res. 28: 717A.

Young, D. F. 1979. Fluid dynamics of arterial stenoses. J. Biomech. Engr. 101:157-175.

Young, D. F., N. R. Cholvin, R. L. Kirkeeide, and A. C. Roth. 1977. Hemodynamics of arterial stenosis at elevated flow rates. Circ. Res. 41:99-107.

ACKNOWLEDGMENTS

This study was conducted at both the University of Iowa and Iowa State University. The initial development and testing of the Doppler balloon catheter was conducted under the supervision of Dr. Carl White at the University of Iowa Hospitals and Clinics. The hemodynamic evaluation portion of the study was conducted under the guidance of Dr. Donald Young from the Biomedical Engineering Program, Iowa State University.

I would like to thank Dr. Carl White, Dr. Donald Young, and Mr. Donald Laughlin for their supervision and invaluable assistance. I would also like to thank Dr. David Carlson and Dr. Fred Hembrough for serving on my committee. In addition, I wish to express my appreciation for the assistance of Dr. Robert Wilson and Dr. John Rumberger.

APPENDIX

The momentum equation was used to evaluate the pressure rise in the expansion region just distal to the tip of the catheter (refer to Figure 13). The basic equation is

$$\Sigma F = \rho Q(\bar{u}_2-\bar{u}_1) \tag{A1}$$

Since

$$\Sigma F = p_1A_0 - p_2A_0 \tag{A2}$$

it follows that

$$p_1A_0-p_2A_0 = \rho Q(\bar{u}_2-\bar{u}_1)$$

and dividing by A_0 yields

$$p_1-p_2 = \rho\bar{u}_2(\bar{u}_1-\bar{u}_2) \tag{A3}$$

The corresponding expression for the pressure, p_2, is

$$p_2 = p_1 + \rho\bar{u}_2(\bar{u}_1-\bar{u}_2) \tag{A4}$$

and since $\bar{u}_1>\bar{u}_2$, then $p_2>p_1$. Therefore, there is a pressure increase in the expansion region distal to the tip of the catheter, It also follows that

$$p_2 = p_0-(p_0-p_1) + \rho\bar{u}_2(\bar{u}_1-\bar{u}_2) \tag{A5}$$

and since

$$\Delta p = p_0-p_1 \simeq p_a-p_1$$

then

$$p_2 = p_0 - \Delta p + \rho\bar{u}_2^2((\bar{u}_1/\bar{u}_2) - 1) \tag{A6}$$

also

$$\bar{u}_1/\bar{u}_2 = A_0/A_a \tag{A7}$$

and therefore

$$p_2 = p_0 - \Delta p + \rho\bar{u}_2^2((A_0/A_a) - 1)$$

application of the Bernoulli equation yields

$$p_0 = p_a + \tfrac{1}{2}\rho(\bar{u}_a^2 - \bar{u}_1^2) \tag{A8}$$

and substituting for p_0

$$p_2 = p_a + \tfrac{1}{2}\rho(\bar{u}_a^2 - \bar{u}_1^2) - \Delta p + \rho\bar{u}_2^2((A_0/A_1) - 1)$$

so that

$$p_a - p_2 = \tfrac{1}{2}\rho(\bar{u}_1^2 - \bar{u}_a) + \Delta p + \rho\bar{u}_2^2(1 - (A_0/A_a)) \tag{A9}$$

and thus

$$p_a - p_2 = A + B + \Delta p \tag{A10}$$

where:

$$A = \tfrac{1}{2}\rho(\bar{u}_1^2 - \bar{u}_2^2)$$

$$B = \rho\bar{u}_2^2(1 - (A_0/A_a))$$

$$\Delta p = p_0 - p_1 \simeq p_a - p_1$$

A+B indicates the sum of the pressure gradient in the expansion region and the pressure gradient in the expansion

region distal to the tip of the catheter, and Δp is the pressure drop, $\Delta p = p_0 - p_1$, in the annular region along the catheter. Thus, $(A+B)/p_a$ indicates the significance of the sum of the pressure gradients in the entrance and expansion regions relative to the pressure drop in the annular region along the catheter. Calculations of $(A+B)/p_a$ have shown the sum of the pressure gradients in the entrance and expansion region to be negligible ($(A+B)/p_a < 0.15$) to the pressure drop in the annular region along the catheter. Therefore the significant pressure gradient is the pressure drop, $\Delta p = p_0 - p_1$, in the annular region along the catheter.